

In Chap. 1 we analyzed the stresses created in various members and connections by the loads applied to a structure or machine. We also learned to design simple members and connections so that they would not fail under specified loading conditions. Another important aspect of the analysis and design of structures relates to the *deformations* caused by the loads applied to a structure. Clearly, it is important to avoid deformations so large that they may prevent the structure from fulfilling the purpose for which it was intended. But the analysis of deformations may also help us in the determination of stresses. Indeed, it is not always possible to determine the forces in the members of a structure by applying only the principles of statics. This is because statics is based on the assumption of undeformable, rigid structures. By considering engineering structures as *deformable* and analyzing the deformations in their various members, it will be possible for us to compute forces that are *statically indeterminate*, i.e., indeterminate within the framework of statics. Also, as we indicated in Sec. 1.5, the distribution of stresses in a given member is statically indeterminate, even when the force in that member is known. To determine the actual distribution of stresses within a member, it is thus necessary to analyze the deformations that take place in that member. In this chapter, you will consider the deformations of a structural member such as a rod, bar, or plate under *axial loading*.

First, the *normal strain* ϵ in a member will be defined as the *deformation of the member per unit length*. Plotting the stress σ versus the strain ϵ as the load applied to the member is increased will yield a *stress-strain diagram* for the material used. From such a diagram we can determine some important properties of the material, such as its *modulus of elasticity*, and whether the material is *ductile* or *brittle* (Secs. 2.2 to 2.5). You will also see in Sec. 2.5 that, while the behavior of most materials is independent of the direction in which the load is applied, the response of fiber-reinforced composite materials depends upon the direction of the load.

From the stress-strain diagram, we can also determine whether the strains in the specimen will disappear after the load has been removed—in which case the material is said to behave *elastically*—or whether a *permanent set* or *plastic deformation* will result (Sec. 2.6).

Section 2.7 is devoted to the phenomenon of *fatigue*, which causes structural or machine components to fail after a very large number of repeated loadings, even though the stresses remain in the elastic range.

The first part of the chapter ends with Sec. 2.8, which is devoted to the determination of the deformation of various types of members under various conditions of axial loading.

In Secs. 2.9 and 2.10, *statically indeterminate problems* will be considered, i.e., problems in which the reactions and the internal forces *cannot* be determined from statics alone. The equilibrium equations derived from the free-body diagram of the member under consideration must be complemented by relations involving deformations; these relations will be obtained from the geometry of the problem.

In Secs. 2.11 to 2.15, additional constants associated with isotropic materials—i.e., materials with mechanical characteristics independent of direction—will be introduced. They include *Poisson's ratio*, which relates

lateral and axial strain, the *bulk modulus*, which characterizes the change in volume of a material under hydrostatic pressure, and the *modulus of rigidity*, which relates the components of the shearing stress and shearing strain. Stress-strain relationships for an isotropic material under a multi-axial loading will also be derived.

In Sec. 2.16, stress-strain relationships involving several distinct values of the modulus of elasticity, Poisson’s ratio, and the modulus of rigidity, will be developed for fiber-reinforced composite materials under a multi-axial loading. While these materials are not isotropic, they usually display special properties, known as *orthotropic* properties, which facilitate their study.

In the text material described so far, stresses are assumed uniformly distributed in any given cross section; they are also assumed to remain within the elastic range. The validity of the first assumption is discussed in Sec. 2.17, while *stress concentrations* near circular holes and fillets in flat bars are considered in Sec. 2.18. Sections 2.19 and 2.20 are devoted to the discussion of stresses and deformations in members made of a ductile material when the yield point of the material is exceeded. As you will see, permanent *plastic deformations* and *residual stresses* result from such loading conditions.

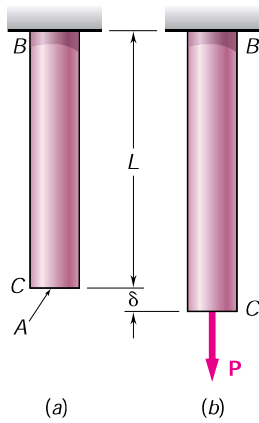


Fig. 2.1

2.2. NORMAL STRAIN UNDER AXIAL LOADING

Let us consider a rod BC , of length L and uniform cross-sectional area A , which is suspended from B (Fig. 2.1a). If we apply a load P to end C , the rod elongates (Fig. 2.1b). Plotting the magnitude P of the load against the deformation δ (Greek letter delta), we obtain a certain load-deformation diagram (Fig. 2.2). While this diagram contains information useful to the analysis of the rod under consideration, it cannot be used directly to predict the deformation of a rod of the same material but of different dimensions. Indeed, we observe that, if a deformation δ is produced in rod BC by a load P , a load $2P$ is required to cause the same deformation in a rod $B'C'$ of the same length L , but of cross-sectional area $2A$ (Fig. 2.3). We note that, in both cases, the value of the stress is the same: $\mathbf{s} = P/A$. On the other hand, a load P applied

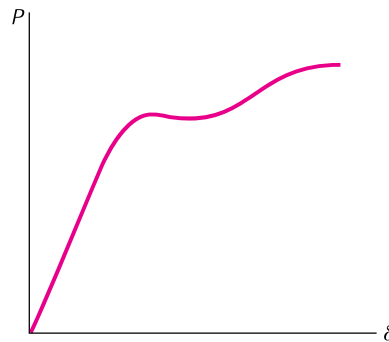


Fig. 2.2

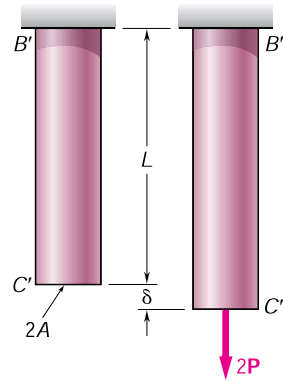


Fig. 2.3

to a rod $B''C''$, of the same cross-sectional area A , but of length $2L$, causes a deformation $2\mathbf{d}$ in that rod (Fig. 2.4), i.e., a deformation twice as large as the deformation \mathbf{d} it produces in rod BC . But in both cases the ratio of the deformation over the length of the rod is the same; it is equal to \mathbf{d}/L . This observation brings us to introduce the concept of *strain*: We define the *normal strain* in a rod under axial loading as the *deformation per unit length* of that rod. Denoting the normal strain by ϵ (Greek letter epsilon), we write

$$\epsilon = \frac{\mathbf{d}}{L} \quad (2.1)$$

Plotting the stress $\mathbf{s} = P/A$ against the strain $\epsilon = \mathbf{d}/L$, we obtain a curve that is characteristic of the properties of the material and does not depend upon the dimensions of the particular specimen used. This curve is called a *stress-strain diagram* and will be discussed in detail in Sec. 2.3.

Since the rod BC considered in the preceding discussion had a uniform cross section of area A , the normal stress \mathbf{s} could be assumed to have a constant value P/A throughout the rod. Thus, it was appropriate to define the strain ϵ as the ratio of the total deformation \mathbf{d} over the total length L of the rod. In the case of a member of variable cross-sectional area A , however, the normal stress $\mathbf{s} = P/A$ varies along the member, and it is necessary to define the strain at a given point Q by considering a small element of undeformed length Δx (Fig. 2.5). Denoting by $\Delta\mathbf{d}$ the deformation of the element under the given loading, we define the *normal strain at point Q* as

$$\epsilon = \lim_{\Delta x \rightarrow 0} \frac{\Delta\mathbf{d}}{\Delta x} = \frac{d\mathbf{d}}{dx} \quad (2.2)$$

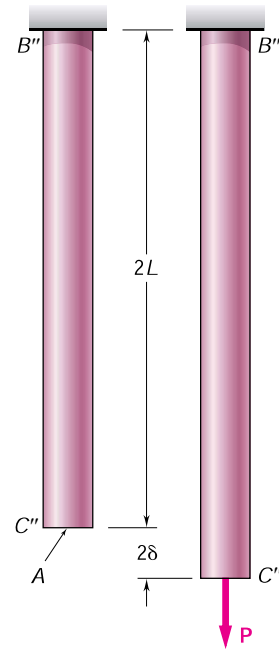


Fig. 2.4

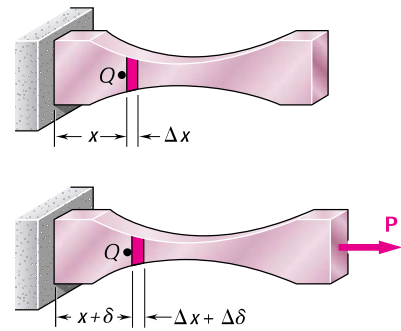


Fig. 2.5

Since deformation and length are expressed in the same units, the normal strain ϵ obtained by dividing \mathbf{d} by L (or $d\mathbf{d}$ by dx) is a *dimensionless quantity*. Thus, the same numerical value is obtained for the normal strain in a given member, whether SI metric units or U.S. customary units are used. Consider, for instance, a bar of length $L = 0.600$ m and uniform cross section, which undergoes a deformation $\mathbf{d} = 150 \times 10^{-6}$ m. The corresponding strain is

$$\epsilon = \frac{\mathbf{d}}{L} = \frac{150 \times 10^{-6} \text{ m}}{0.600 \text{ m}} = 250 \times 10^{-6} \text{ m/m} = 250 \times 10^{-6}$$

Note that the deformation could have been expressed in micrometers: $\mathbf{d} = 150 \text{ }\mu\text{m}$. We would then have written

$$\epsilon = \frac{\mathbf{d}}{L} = \frac{150 \text{ }\mu\text{m}}{0.600 \text{ m}} = 250 \text{ }\mu\text{m/m} = 250 \text{ }\mu$$

and read the answer as “250 micros.” If U.S. customary units are used, the length and deformation of the same bar are, respectively, $L = 23.6$ in. and $\mathbf{d} = 5.91 \times 10^{-3}$ in. The corresponding strain is

$$\epsilon = \frac{\mathbf{d}}{L} = \frac{5.91 \times 10^{-3} \text{ in.}}{23.6 \text{ in.}} = 250 \times 10^{-6} \text{ in./in.}$$

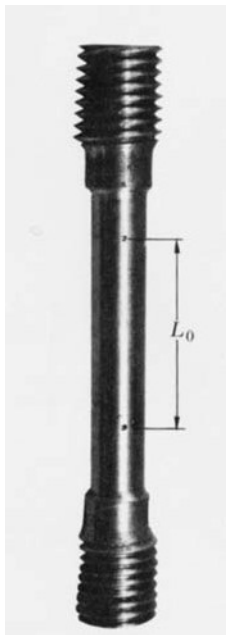


Fig. 2.6 Typical tensile-test specimen.

which is the same value that we found using SI units. It is customary, however, when lengths and deformations are expressed in inches or micro-inches ($\mu\text{in.}$), to keep the original units in the expression obtained for the strain. Thus, in our example, the strain would be recorded as $\epsilon = 250 \times 10^{-6}$ in./in. or, alternatively, as $\epsilon = 250 \text{ }\mu\text{in./in.}$

2.3. STRESS-STRAIN DIAGRAM

We saw in Sec. 2.2 that the diagram representing the relation between stress and strain in a given material is an important characteristic of the material. To obtain the stress-strain diagram of a material, one usually conducts a *tensile test* on a specimen of the material. One type of specimen commonly used is shown in Fig. 2.6. The cross-sectional area of the cylindrical central portion of the specimen has been accurately determined and two gage marks have been inscribed on that portion at a distance L_0 from each other. The distance L_0 is known as the *gage length* of the specimen.

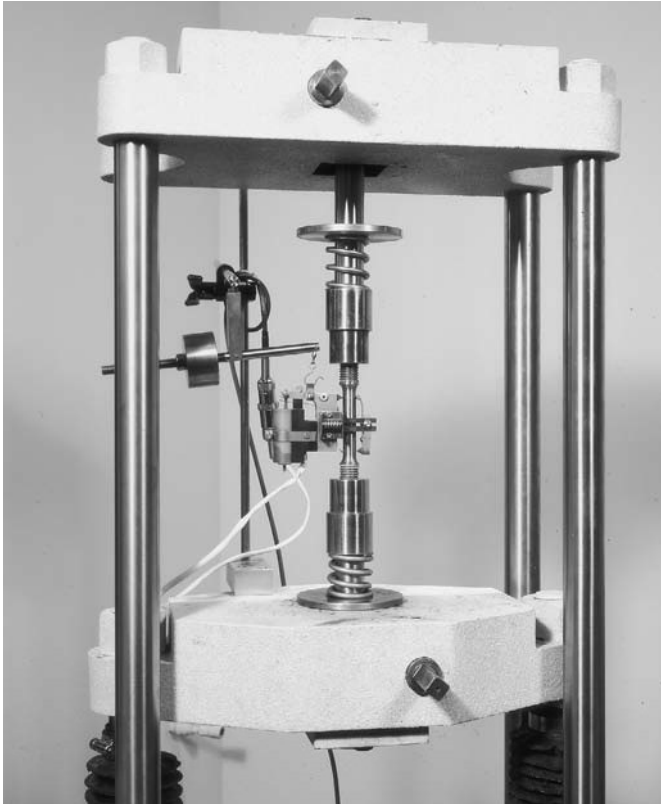


Fig. 2.7 This machine is used to test tensile test specimens, such as those shown in this chapter.

The test specimen is then placed in a testing machine (Fig. 2.7), which is used to apply a centric load P . As the load P increases, the distance L between the two gage marks also increases (Fig. 2.8). The distance L is measured with a dial gage, and the elongation $\mathbf{d} = L - L_0$ is recorded for each value of P . A second dial gage is often used simultaneously to measure and record the change in diameter of the specimen. From each pair of readings P and \mathbf{d} , the stress \mathbf{s} is computed by dividing P by the original cross-sectional area A_0 of the specimen, and the strain ϵ by dividing the elongation \mathbf{d} by the original distance L_0 between the two gage marks. The stress-strain diagram may then be obtained by plotting ϵ as an abscissa and \mathbf{s} as an ordinate.

Stress-strain diagrams of various materials vary widely, and different tensile tests conducted on the same material may yield different results, depending upon the temperature of the specimen and the speed of loading. It is possible, however, to distinguish some common characteristics among the stress-strain diagrams of various groups of materials and to divide materials into two broad categories on the basis of these characteristics, namely, the *ductile* materials and the *brittle* materials.

Ductile materials, which comprise structural steel, as well as many alloys of other metals, are characterized by their ability to *yield* at normal temperatures. As the specimen is subjected to an increasing load, its length first increases linearly with the load and at a very slow rate. Thus, the initial portion of the stress-strain diagram is a straight line

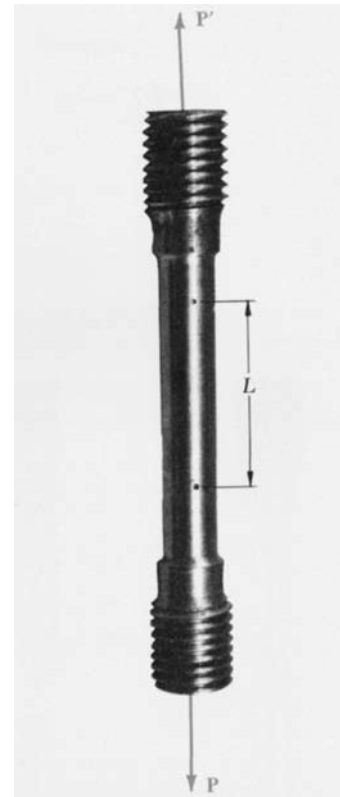


Fig. 2.8 Test specimen with tensile load.

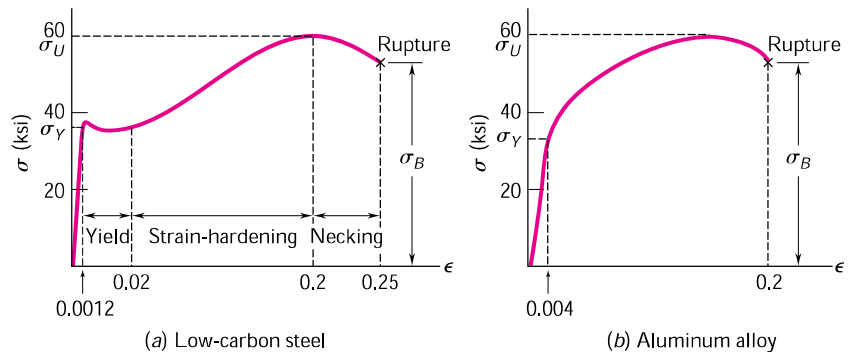


Fig. 2.9 Stress-strain diagrams of two typical ductile materials.

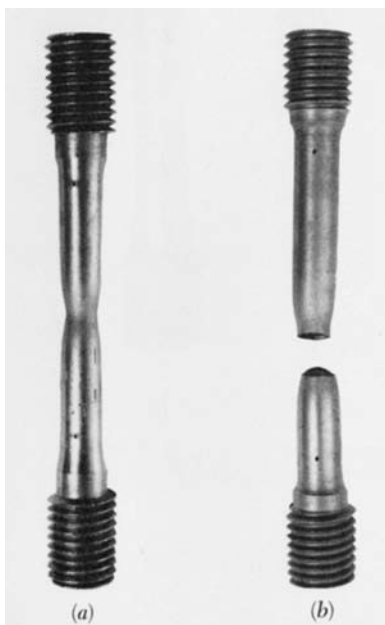


Fig. 2.10 Tested specimen of a ductile material.

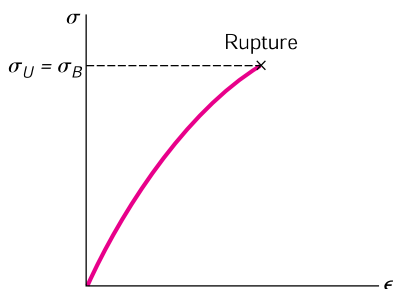


Fig. 2.11 Stress-strain diagram for a typical brittle material.

with a steep slope (Fig. 2.9). However, after a critical value σ_Y of the stress has been reached, the specimen undergoes a large deformation with a relatively small increase in the applied load. This deformation is caused by slippage of the material along oblique surfaces and is due, therefore, primarily to shearing stresses. As we can note from the stress-strain diagrams of two typical ductile materials (Fig. 2.9), the elongation of the specimen after it has started to yield can be 200 times as large as its deformation before yield. After a certain maximum value of the load has been reached, the diameter of a portion of the specimen begins to decrease, because of local instability (Fig. 2.10a). This phenomenon is known as *necking*. After necking has begun, somewhat lower loads are sufficient to keep the specimen elongating further, until it finally ruptures (Fig. 2.10b). We note that rupture occurs along a cone-shaped surface that forms an angle of approximately 45° with the original surface of the specimen. This indicates that shear is primarily responsible for the failure of ductile materials, and confirms the fact that, under an axial load, shearing stresses are largest on surfaces forming an angle of 45° with the load (cf. Sec. 1.11). The stress σ_Y at which yield is initiated is called the *yield strength* of the material, the stress σ_U corresponding to the maximum load applied to the specimen is known as the *ultimate strength*, and the stress σ_B corresponding to rupture is called the *breaking strength*.

Brittle materials, which comprise cast iron, glass, and stone, are characterized by the fact that rupture occurs without any noticeable prior change in the rate of elongation (Fig. 2.11). Thus, for brittle materials, there is no difference between the ultimate strength and the breaking strength. Also, the strain at the time of rupture is much smaller for brittle than for ductile materials. From Fig. 2.12, we note the absence of any necking of the specimen in the case of a brittle material, and observe that rupture occurs along a surface perpendicular to the load. We conclude from this observation that normal stresses are primarily responsible for the failure of brittle materials.†

†The tensile tests described in this section were assumed to be conducted at normal temperatures. However, a material that is ductile at normal temperatures may display the characteristics of a brittle material at very low temperatures, while a normally brittle material may behave in a ductile fashion at very high temperatures. At temperatures other than normal, therefore, one should refer to a material in a ductile state or to a material in a brittle state, rather than to a ductile or brittle material.

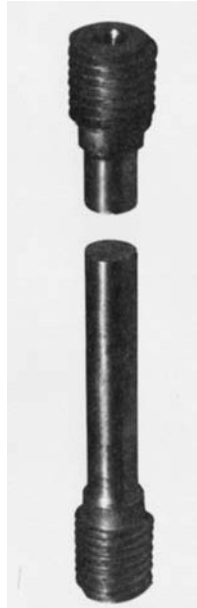


Fig. 2.12 Tested specimen of a brittle material.

The stress-strain diagrams of Fig. 2.9 show that structural steel and aluminum, while both ductile, have different yield characteristics. In the case of structural steel (Fig. 2.9a), the stress remains constant over a large range of values of the strain after the onset of yield. Later the stress must be increased to keep elongating the specimen, until the maximum value σ_U has been reached. This is due to a property of the material known as strain-hardening. The yield strength of structural steel can be determined during the tensile test by watching the load shown on the display of the testing machine. After increasing steadily, the load is observed to suddenly drop to a slightly lower value, which is maintained for a certain period while the specimen keeps elongating. In a very carefully conducted test, one may be able to distinguish between the *upper yield point*, which corresponds to the load reached just before yield starts, and the *lower yield point*, which corresponds to the load required to maintain yield. Since the upper yield point is transient, the lower yield point should be used to determine the yield strength of the material.

In the case of aluminum (Fig. 2.9b) and of many other ductile materials, the onset of yield is not characterized by a horizontal portion of the stress-strain curve. Instead, the stress keeps increasing—although not linearly—until the ultimate strength is reached. Necking then begins, leading eventually to rupture. For such materials, the yield strength σ_Y can be defined by the offset method. The yield strength at 0.2% offset, for example, is obtained by drawing through the point of the horizontal axis of abscissa $\epsilon = 0.2\%$ (or $\epsilon = 0.002$), a line parallel to the initial straight-line portion of the stress-strain diagram (Fig. 2.13). The stress σ_Y corresponding to the point Y obtained in this fashion is defined as the yield strength at 0.2% offset.

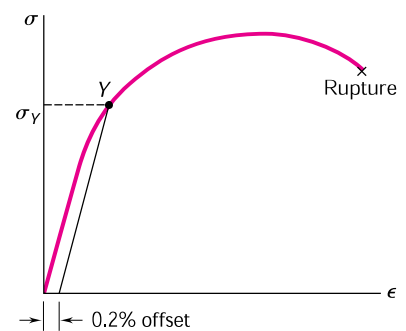


Fig. 2.13 Determination of yield strength by offset method.

A standard measure of the ductility of a material is its *percent elongation*, which is defined as

$$\text{Percent elongation} = 100 \frac{L_B - L_0}{L_0}$$

where L_0 and L_B denote, respectively, the initial length of the tensile test specimen and its final length at rupture. The specified minimum elongation for a 2-in. gage length for commonly used steels with yield strengths up to 50 ksi is 21%. We note that this means that the average strain at rupture should be at least 0.21 in./in.

Another measure of ductility which is sometimes used is the *percent reduction in area*, defined as

$$\text{Percent reduction in area} = 100 \frac{A_0 - A_B}{A_0}$$

where A_0 and A_B denote, respectively, the initial cross-sectional area of the specimen and its minimum cross-sectional area at rupture. For structural steel, percent reductions in area of 60 to 70 percent are common.

Thus far, we have discussed only tensile tests. If a specimen made of a ductile material were loaded in compression instead of tension, the stress-strain curve obtained would be essentially the same through its initial straight-line portion and through the beginning of the portion corresponding to yield and strain-hardening. Particularly noteworthy is the fact that for a given steel, the yield strength is the same in both tension and compression. For larger values of the strain, the tension and compression stress-strain curves diverge, and it should be noted that necking cannot occur in compression. For most brittle materials, one finds that the ultimate strength in compression is much larger than the ultimate strength in tension. This is due to the presence of flaws, such as microscopic cracks or cavities, which tend to weaken the material in tension, while not appreciably affecting its resistance to compressive failure.

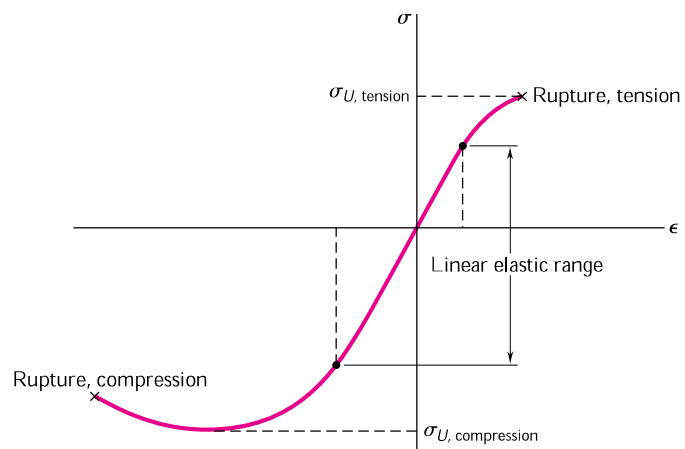


Fig. 2.14 Stress-strain diagram for concrete.

An example of brittle material with different properties in tension and compression is provided by *concrete*, whose stress-strain diagram is shown in Fig. 2.14. On the tension side of the diagram, we first observe a linear elastic range in which the strain is proportional to the stress. After the yield point has been reached, the strain increases faster than the stress until rupture occurs. The behavior of the material in compression is different. First, the linear elastic range is significantly larger. Second, rupture does not occur as the stress reaches its maximum value. Instead, the stress decreases in magnitude while the strain keeps increasing until rupture occurs. Note that the modulus of elasticity, which is represented by the slope of the stress-strain curve in its linear portion, is the same in tension and compression. This is true of most brittle materials.

*2.4. TRUE STRESS AND TRUE STRAIN

We recall that the stress plotted in the diagrams of Figs. 2.9 and 2.11 was obtained by dividing the load P by the cross-sectional area A_0 of the specimen measured before any deformation had taken place. Since the cross-sectional area of the specimen decreases as P increases, the stress plotted in our diagrams does not represent the actual stress in the specimen. The difference between the *engineering stress* $\mathbf{s} = P/A_0$ that we have computed and the *true stress* $\mathbf{s}_t = P/A$ obtained by dividing P by the cross-sectional area A of the deformed specimen becomes apparent in ductile materials after yield has started. While the engineering stress \mathbf{s} , which is directly proportional to the load P , decreases with P during the necking phase, the true stress \mathbf{s}_t , which is proportional to P but also inversely proportional to A , is observed to keep increasing until rupture of the specimen occurs.

Many scientists also use a definition of strain different from that of the *engineering strain* $\epsilon = \mathbf{d}/L_0$. Instead of using the total elongation \mathbf{d} and the original value L_0 of the gage length, they use all the successive values of L that they have recorded. Dividing each increment ΔL of the distance between the gage marks, by the corresponding value of L , they obtain the elementary strain $\Delta\epsilon = \Delta L/L$. Adding the successive values of $\Delta\epsilon$, they define the *true strain* ϵ_t :

$$\epsilon_t = \sum \Delta\epsilon = \sum (\Delta L/L)$$

With the summation replaced by an integral, they can also express the true strain as follows:

$$\epsilon_t = \int_{L_0}^L \frac{dL}{L} = \ln \frac{L}{L_0} \quad (2.3)$$

The diagram obtained by plotting true stress versus true strain (Fig. 2.15) reflects more accurately the behavior of the material. As we have already noted, there is no decrease in true stress during the necking phase. Also, the results obtained from tensile and from compressive

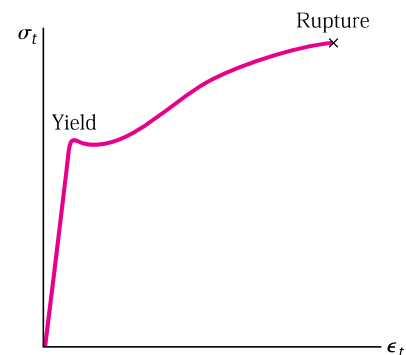


Fig. 2.15 True stress versus true strain for a typical ductile material.

tests will yield essentially the same plot when true stress and true strain are used. This is not the case for large values of the strain when the engineering stress is plotted versus the engineering strain. However, engineers, whose responsibility is to determine whether a load P will produce an acceptable stress and an acceptable deformation in a given member, will want to use a diagram based on the engineering stress $\mathbf{s} = P/A_0$ and the engineering strain $\epsilon = \mathbf{d}/L_0$, since these expressions involve data that are available to them, namely the cross-sectional area A_0 and the length L_0 of the member in its undeformed state.

2.5. HOOKE'S LAW; MODULUS OF ELASTICITY

Most engineering structures are designed to undergo relatively small deformations, involving only the straight-line portion of the corresponding stress-strain diagram. For that initial portion of the diagram (Fig. 2.9), the stress \mathbf{s} is directly proportional to the strain ϵ , and we can write

$$\mathbf{s} = E \epsilon \quad (2.4)$$

This relation is known as *Hooke's law*, after the English mathematician Robert Hooke (1635–1703). The coefficient E is called the *modulus of elasticity* of the material involved, or also *Young's modulus*, after the English scientist Thomas Young (1773–1829). Since the strain ϵ is a dimensionless quantity, the modulus E is expressed in the same units as the stress \mathbf{s} , namely in pascals or one of its multiples if SI units are used, and in psi or ksi if U.S. customary units are used.

The largest value of the stress for which Hooke's law can be used for a given material is known as the *proportional limit* of that material. In the case of ductile materials possessing a well-defined yield point, as in Fig. 2.9a, the proportional limit almost coincides with the yield point. For other materials, the proportional limit cannot be defined as easily, since it is difficult to determine with accuracy the value of the stress \mathbf{s} for which the relation between \mathbf{s} and ϵ ceases to be linear. But from this very difficulty we can conclude for such materials that using Hooke's law for values of the stress slightly larger than the actual proportional limit will not result in any significant error.

Some of the physical properties of structural metals, such as strength, ductility, and corrosion resistance, can be greatly affected by alloying, heat treatment, and the manufacturing process used. For example, we note from the stress-strain diagrams of pure iron and of three different grades of steel (Fig. 2.16) that large variations in the yield strength, ultimate strength, and final strain (ductility) exist among these four metals. All of them, however, possess the same modulus of elasticity; in other words, their "stiffness," or ability to resist a deformation within the linear range, is the same. Therefore, if a high-strength steel is substituted for a lower-strength steel in a given structure, and if all dimensions are kept the same, the structure will have an increased load-carrying capacity, but its stiffness will remain unchanged.

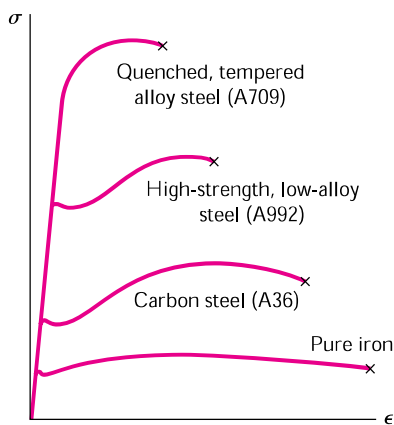


Fig. 2.16 Stress-strain diagrams for iron and different grades of steel.

For each of the materials considered so far, the relation between normal stress and normal strain, $\mathbf{s} = E\epsilon$, is independent of the direction of loading. This is because the mechanical properties of each material, including its modulus of elasticity E , are independent of the direction considered. Such materials are said to be *isotropic*. Materials whose properties depend upon the direction considered are said to be *anisotropic*. An important class of anisotropic materials consists of *fiber-reinforced composite materials*.

These composite materials are obtained by embedding fibers of a strong, stiff material into a weaker, softer material, referred to as a *matrix*. Typical materials used as fibers are graphite, glass, and polymers, while various types of resins are used as a matrix. Figure 2.17 shows a layer, or *lamina*, of a composite material consisting of a large number of parallel fibers embedded in a matrix. An axial load applied to the lamina along the x axis, that is, in a direction parallel to the fibers, will create a normal stress \mathbf{s}_x in the lamina and a corresponding normal strain ϵ_x which will satisfy Hooke's law as the load is increased and as long as the elastic limit of the lamina is not exceeded. Similarly, an axial load applied along the y axis, that is, in a direction perpendicular to the lamina, will create a normal stress \mathbf{s}_y and a normal strain ϵ_y , satisfying Hooke's law, and an axial load applied along the z axis will create a normal stress \mathbf{s}_z and a normal strain ϵ_z which again satisfy Hooke's law. However, the moduli of elasticity E_x , E_y , and E_z corresponding, respectively, to each of the above loadings will be different. Because the fibers are parallel to the x axis, the lamina will offer a much stronger resistance to a loading directed along the x axis than to a loading directed along the y or z axis, and E_x will be much larger than either E_y or E_z .

A flat *laminata* is obtained by superposing a number of layers or laminae. If the laminata is to be subjected only to an axial load causing tension, the fibers in all layers should have the same orientation as the load in order to obtain the greatest possible strength. But if the laminata may be in compression, the matrix material may not be sufficiently strong to prevent the fibers from kinking or buckling. The lateral stability of the laminata may then be increased by positioning some of the layers so that their fibers will be perpendicular to the load. Positioning some layers so that their fibers are oriented at 30° , 45° , or 60° to the load may also be used to increase the resistance of the laminata to in-plane shear. Fiber-reinforced composite materials will be further discussed in Sec. 2.16, where their behavior under multiaxial loadings will be considered.

2.6. ELASTIC VERSUS PLASTIC BEHAVIOR OF A MATERIAL

If the strains caused in a test specimen by the application of a given load disappear when the load is removed, the material is said to behave *elastically*. The largest value of the stress for which the material behaves elastically is called the *elastic limit* of the material.

If the material has a well-defined yield point as in Fig. 2.9a, the elastic limit, the proportional limit (Sec. 2.5), and the yield point are essentially equal. In other words, the material behaves elastically and

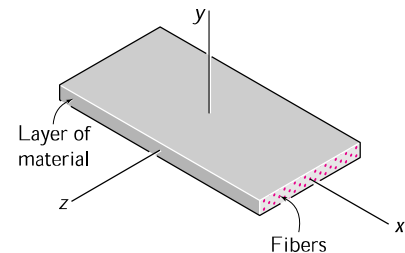


Fig. 2.17 Layer of fiber-reinforced composite material.

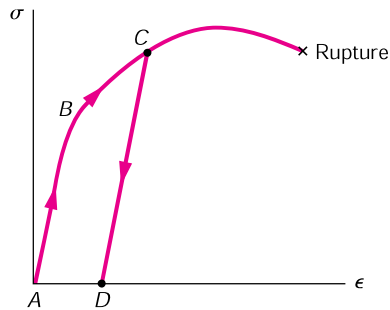


Fig. 2.18

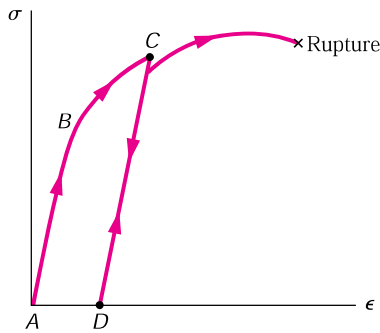


Fig. 2.19

linearly as long as the stress is kept below the yield point. If the yield point is reached, however, yield takes place as described in Sec. 2.3 and, when the load is removed, the stress and strain decrease in a linear fashion, along a line CD parallel to the straight-line portion AB of the loading curve (Fig. 2.18). The fact that ϵ does not return to zero after the load has been removed indicates that a *permanent set* or *plastic deformation* of the material has taken place. For most materials, the plastic deformation depends not only upon the maximum value reached by the stress, but also upon the time elapsed before the load is removed. The stress-dependent part of the plastic deformation is referred to as *slip*, and the time-dependent part—which is also influenced by the temperature—as *creep*.

When a material does not possess a well-defined yield point, the elastic limit cannot be determined with precision. However, assuming the elastic limit equal to the yield strength as defined by the offset method (Sec. 2.3) results in only a small error. Indeed, referring to Fig. 2.13, we note that the straight line used to determine point Y also represents the unloading curve after a maximum stress \mathbf{s}_y has been reached. While the material does not behave truly elastically, the resulting plastic strain is as small as the selected offset.

If, after being loaded and unloaded (Fig. 2.19), the test specimen is loaded again, the new loading curve will closely follow the earlier unloading curve until it almost reaches point C ; it will then bend to the right and connect with the curved portion of the original stress-strain diagram. We note that the straight-line portion of the new loading curve is longer than the corresponding portion of the initial one. Thus, the proportional limit and the elastic limit have increased as a result of the strain-hardening that occurred during the earlier loading of the specimen. However, since the point of rupture R remains unchanged, the ductility of the specimen, which should now be measured from point D , has decreased.

We have assumed in our discussion that the specimen was loaded twice in the same direction, i.e., that both loads were tensile loads. Let us now consider the case when the second load is applied in a direction opposite to that of the first one.

We assume that the material is mild steel, for which the yield strength is the same in tension and in compression. The initial load is tensile and is applied until point C has been reached on the stress-strain diagram (Fig. 2.20). After unloading (point D), a compressive load is applied, causing the material to reach point H , where the stress is equal to $-\mathbf{s}_y$. We note that portion DH of the stress-strain diagram is curved and does not show any clearly defined yield point. This is referred to as the *Bauschinger effect*. As the compressive load is maintained, the material yields along line HJ .

If the load is removed after point J has been reached, the stress returns to zero along line JK , and we note that the slope of JK is equal to the modulus of elasticity E . The resulting permanent set AK may be positive, negative, or zero, depending upon the lengths of the segments BC and HJ . If a tensile load is applied again to the test specimen, the portion of the stress-strain diagram beginning at K (dashed line) will curve up and to the right until the yield stress \mathbf{s}_y has been reached.

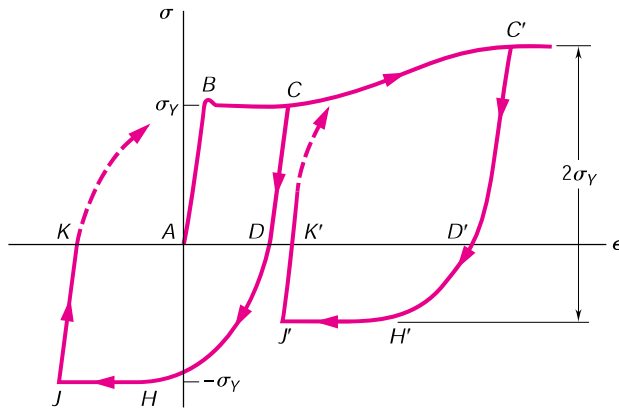


Fig. 2.20

If the initial loading is large enough to cause strain-hardening of the material (point C'), unloading takes place along line $C'D'$. As the reverse load is applied, the stress becomes compressive, reaching its maximum value at H' and maintaining it as the material yields along line $H'J'$. We note that while the maximum value of the compressive stress is less than σ_y , the total change in stress between C' and H' is still equal to $2\sigma_y$.

If point K or K' coincides with the origin A of the diagram, the permanent set is equal to zero, and the specimen may appear to have returned to its original condition. However, internal changes will have taken place and, while the same loading sequence may be repeated, the specimen will rupture without any warning after relatively few repetitions. This indicates that the excessive plastic deformations to which the specimen was subjected have caused a radical change in the characteristics of the material. Reverse loadings into the plastic range, therefore, are seldom allowed, and only under carefully controlled conditions. Such situations occur in the straightening of damaged material and in the final alignment of a structure or machine.

2.7. REPEATED LOADINGS; FATIGUE

In the preceding sections we have considered the behavior of a test specimen subjected to an axial loading. We recall that, if the maximum stress in the specimen does not exceed the elastic limit of the material, the specimen returns to its initial condition when the load is removed. You might conclude that a given loading may be repeated many times, provided that the stresses remain in the elastic range. Such a conclusion is correct for loadings repeated a few dozen or even a few hundred times. However, as you will see, it is not correct when loadings are repeated thousands or millions of times. In such cases, rupture will occur at a stress much lower than the static breaking strength; this phenomenon is known as *fatigue*. A fatigue failure is of a brittle nature, even for materials that are normally ductile.

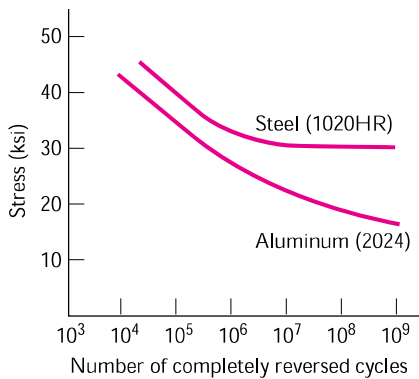


Fig. 2.21

Fatigue must be considered in the design of all structural and machine components that are subjected to repeated or to fluctuating loads. The number of loading cycles that may be expected during the useful life of a component varies greatly. For example, a beam supporting an industrial crane may be loaded as many as two million times in 25 years (about 300 loadings per working day), an automobile crankshaft will be loaded about half a billion times if the automobile is driven 200,000 miles, and an individual turbine blade may be loaded several hundred billion times during its lifetime.

Some loadings are of a fluctuating nature. For example, the passage of traffic over a bridge will cause stress levels that will fluctuate about the stress level due to the weight of the bridge. A more severe condition occurs when a complete reversal of the load occurs during the loading cycle. The stresses in the axle of a railroad car, for example, are completely reversed after each half-revolution of the wheel.

The number of loading cycles required to cause the failure of a specimen through repeated successive loadings and reverse loadings may be determined experimentally for any given maximum stress level. If a series of tests is conducted, using different maximum stress levels, the resulting data may be plotted as a s - n curve. For each test, the maximum stress s is plotted as an ordinate and the number of cycles n as an abscissa; because of the large number of cycles required for rupture, the cycles n are plotted on a logarithmic scale.

A typical s - n curve for steel is shown in Fig. 2.21. We note that, if the applied maximum stress is high, relatively few cycles are required to cause rupture. As the magnitude of the maximum stress is reduced, the number of cycles required to cause rupture increases, until a stress, known as the *endurance limit*, is reached. The endurance limit is the stress for which failure does not occur, even for an indefinitely large number of loading cycles. For a low-carbon steel, such as structural steel, the endurance limit is about one-half of the ultimate strength of the steel.

For nonferrous metals, such as aluminum and copper, a typical s - n curve (Fig. 2.21) shows that the stress at failure continues to decrease as the number of loading cycles is increased. For such metals, one defines the *fatigue limit* as the stress corresponding to failure after a specified number of loading cycles, such as 500 million.

Examination of test specimens, of shafts, of springs, and of other components that have failed in fatigue shows that the failure was initiated at a microscopic crack or at some similar imperfection. At each loading, the crack was very slightly enlarged. During successive loading cycles, the crack propagated through the material until the amount of undamaged material was insufficient to carry the maximum load, and an abrupt, brittle failure occurred. Because fatigue failure may be initiated at any crack or imperfection, the surface condition of a specimen has an important effect on the value of the endurance limit obtained in testing. The endurance limit for machined and polished specimens is higher than for rolled or forged components, or for components that are corroded. In applications in or near seawater, or in other applications where corrosion is expected, a reduction of up to 50% in the endurance limit can be expected.

2.8. DEFORMATIONS OF MEMBERS UNDER AXIAL LOADING

Consider a homogeneous rod BC of length L and uniform cross section of area A subjected to a centric axial load \mathbf{P} (Fig. 2.22). If the resulting axial stress $\mathbf{s} = P/A$ does not exceed the proportional limit of the material, we may apply Hooke's law and write

$$\mathbf{s} = E \epsilon \quad (2.4)$$

from which it follows that

$$\epsilon = \frac{\mathbf{s}}{E} = \frac{P}{AE} \quad (2.5)$$

Recalling that the strain ϵ was defined in Sec. 2.2 as $\epsilon = \mathbf{d}/L$, we have

$$\mathbf{d} = \epsilon L \quad (2.6)$$

and, substituting for ϵ from (2.5) into (2.6):

$$\mathbf{d} = \frac{PL}{AE} \quad (2.7)$$

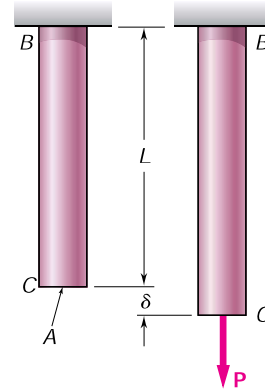


Fig. 2.22

Equation (2.7) may be used only if the rod is homogeneous (constant E), has a uniform cross section of area A , and is loaded at its ends. If the rod is loaded at other points, or if it consists of several portions of various cross sections and possibly of different materials, we must divide it into component parts that satisfy individually the required conditions for the application of formula (2.7). Denoting, respectively, by P_i , L_i , A_i , and E_i the internal force, length, cross-sectional area, and modulus of elasticity corresponding to part i , we express the deformation of the entire rod as

$$\mathbf{d} = \sum_i \frac{P_i L_i}{A_i E_i} \quad (2.8)$$

We recall from Sec. 2.2 that, in the case of a rod of variable cross section (Fig. 2.5), the strain ϵ depends upon the position of the point Q where it is computed and is defined as $\epsilon = d\mathbf{d}/dx$. Solving for $d\mathbf{d}$ and substituting for ϵ from Eq. (2.5), we express the deformation of an element of length dx as

$$d\mathbf{d} = \epsilon dx = \frac{P dx}{AE}$$

The total deformation \mathbf{d} of the rod is obtained by integrating this expression over the length L of the rod:

$$\mathbf{d} = \int_0^L \frac{P dx}{AE} \quad (2.9)$$

Formula (2.9) should be used in place of (2.7), not only when the cross-sectional area A is a function of x , but also when the internal force P depends upon x , as is the case for a rod hanging under its own weight.

EXAMPLE 2.01

Determine the deformation of the steel rod shown in Fig. 2.23a under the given loads ($E = 29 \times 10^6$ psi).

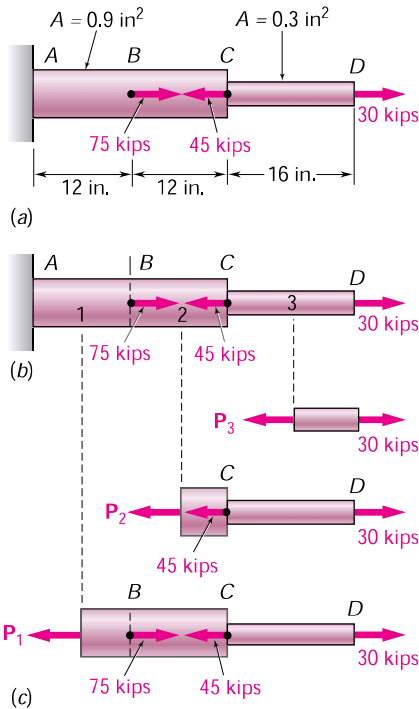


Fig. 2.23

We divide the rod into three component parts shown in Fig. 2.23b and write

$$L_1 = L_2 = 12 \text{ in.} \quad L_3 = 16 \text{ in.}$$

$$A_1 = A_2 = 0.9 \text{ in}^2 \quad A_3 = 0.3 \text{ in}^2$$

To find the internal forces P_1 , P_2 , and P_3 , we must pass sections through each of the component parts, drawing each time the free-body diagram of the portion of rod located to the right of the section (Fig. 2.23c). Expressing that each of the free bodies is in equilibrium, we obtain successively

$$P_1 = 60 \text{ kips} = 60 \times 10^3 \text{ lb}$$

$$P_2 = -15 \text{ kips} = -15 \times 10^3 \text{ lb}$$

$$P_3 = 30 \text{ kips} = 30 \times 10^3 \text{ lb}$$

Carrying the values obtained into Eq. (2.8), we have

$$\mathbf{d} = \sum_i \frac{P_i L_i}{A_i E_i} = \frac{1}{E} \left(\frac{P_1 L_1}{A_1} + \frac{P_2 L_2}{A_2} + \frac{P_3 L_3}{A_3} \right)$$

$$= \frac{1}{29 \times 10^6} \left[\frac{(60 \times 10^3)(12)}{0.9} + \frac{(-15 \times 10^3)(12)}{0.9} + \frac{(30 \times 10^3)(16)}{0.3} \right]$$

$$\mathbf{d} = \frac{2.20 \times 10^6}{29 \times 10^6} = 75.9 \times 10^{-3} \text{ in.}$$

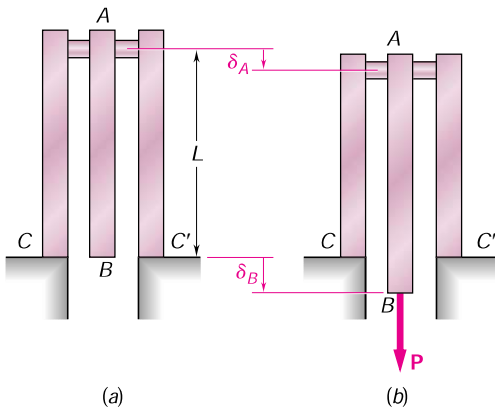


Fig. 2.24

The rod BC of Fig. 2.22, which was used to derive formula (2.7), and the rod AD of Fig. 2.23, which has just been discussed in Example 2.01, both had one end attached to a fixed support. In each case, therefore, the deformation \mathbf{d} of the rod was equal to the displacement of its free end. When both ends of a rod move, however, the deformation of the rod is measured by the *relative displacement* of one end of the rod with respect to the other. Consider, for instance, the assembly shown in Fig. 2.24a, which consists of three elastic bars of length L connected by a rigid pin at A . If a load \mathbf{P} is applied at B (Fig. 2.24b), each of the three bars will deform. Since the bars AC and AC' are attached to fixed supports at C and C' , their common deformation is measured by the displacement \mathbf{d}_A of point A . On the other hand, since both ends of bar AB move, the deformation of AB is measured by the difference between the displacements \mathbf{d}_A and \mathbf{d}_B of points A and B , i.e., by the relative displacement of B with respect to A . Denoting this relative displacement by $\mathbf{d}_{B/A}$, we write

$$\mathbf{d}_{B/A} = \mathbf{d}_B - \mathbf{d}_A = \frac{PL}{AE} \quad (2.10)$$

where A is the cross-sectional area of AB and E is its modulus of elasticity.